Available online at www.sciencedirect.com
SCIENCE DIRECT
Journal of Catalysis 241 (2006) 319–327
JOURNAL OF CATALYSIS
www.elsevier.com/locate/jcat

An effective heterogeneous L-proline catalyst for the asymmetric aldol reaction using anionic clays as intercalated support

Zhe An, Wenhui Zhang, Huimin Shi, Jing He *

State Key Laboratory of Chemical Resource Engineering, Beijing University of Chemical Technology, Beijing 100029, PR China

Received 27 February 2006; revised 28 April 2006; accepted 28 April 2006

Available online 9 June 2006

Abstract

A heterogeneous catalyst (L-Pro LDHs) was developed using intercalation of L-proline in Mg–Al LDH. An investigation of the thermal stability and optical stability showed that the immobilization of the chiral catalytic centers in restricted galleries enhanced the enantiomeric stability against thermal treatment and light irradiation. Asymmetric aldol reaction of benzaldehyde and acetone was carried out using L-Pro LDHs as catalyst, resulting in a good yield (90%) and a high enantiomeric excess (94%). The enantiomeric selectivity of L-Pro LDHs was found to be more stable to thermal pretreatment compared with the pristine L-proline. The possible reaction mechanism was proposed in light of the homogeneous mechanism. The effects of chemical composition of L-Pro LDHs and reaction conditions on catalytic efficiency were also investigated.

Keywords: L-Proline; Layered double hydroxides; Heterogeneous catalysts; Asymmetric aldol reaction; Optical stability; Enantiomeric selectivity

1. Introduction

Due to economic, environmental, and social factors, the application of optically pure compounds is dramatically increasing [1]. Among the various methods of selectively producing single enantiomers, asymmetric catalysis is one of the most attractive methods from an atom-economic standpoint. It is well known that the asymmetric aldol reaction is one of the most important C–C bond-forming reactions in organic synthesis and is of much importance in the pharmaceutical, agrochemical, and fine chemical industries [2]. The design and preparation of highly selective asymmetric catalysts for the aldol reaction has hence attracted much attention [3–9].

Proline [10,11], an important useful chiral amino acid, has been applied to catalyze the enantioselective asymmetric aldol process due to its special structure and properties. Recently, a renewed interest in its use for the biomimetic approach to catalytic asymmetric C–C bond-forming reactions is increasing [12–14]. Proline derivatives have also been synthesized in an attempt to enhance enantioselectivity [15–17]. Due to the unavoidable drawbacks of homogeneous catalytic processes (e.g., short lifetime, lower structural and thermal stability, and difficulties in catalyst separation and recovery), as well as concerns about product purity [18], the immobilization of L-proline has been widely investigated on inorganic supports, including mesoporous materials [19,20], metals [21,22], and layered compounds [23].

Layered double hydroxides (LDHs), also known as hydrotalcite-like compounds, are a class of synthetic anionic layered clays that can be represented by the general formula $[M^{II}_{1-x}M^{III}_{x}(OH)_2]^{x+}(A^{n-})_{x/n}\cdot yH_2O$ [24]. Their structure is based on brucite-like layers, where a divalent metal cation is located in the center of oxygen octahedra and two-dimensional infinite layers are formed by edge-sharing of octahedra. The partial isomorphous substitution of trivalent cations for divalent ones results in a positive charge on the layers, and the interlayer A^{n-} anions balance the charge. Several synthetical methods are available [25–29] to introduce anions as guests into the interlayers of LDHs, among which the reconstruction method, related to its "memory effect," has been extensively used for the preparation of organo-LDHs [30]. Calcination of LDHs at a certain temperature [31] removes the interlayer water, interlayer anions, and hydroxyl groups, resulting in a mixed metal oxide

* Corresponding author. Fax: +86 10 64425385.
E-mail address: jinghe@263.net.cn (J. He).

0021-9517/$ – see front matter
doi:10.1016/j.jcat.2006.04.035

(LDO) that cannot be achieved by mechanical means. It is especially interesting that the calcined LDH is able to regenerate the layered structure when exposed to water and anions. The incorporated anions do not necessarily need to be the same anion as in the original LDH material; thus this represents an interesting method for intercalating various inorganic and organic anion forms within the LDHs layers, as well as pillared structures [32].

In recent years, the preparation of L-Pro LDHs through ion-exchange method [23] and their application in asymmetric aldol reactions with relatively good yield have been studied, but especially low enantiomeric excess (ee%) was achieved. The immobilization of L-proline [33] on LDHs by the reconstruction method was also studied, but no catalytic performance was presented. Herein we present a detailed investigation of the preparation and characterization of L-proline intercalated into LDHs (L-Pro LDHs) by the "memory effect," along with its application in a typical aldol reaction between acetone and benzaldehyde. High yield and high ee are achieved. The catalytic activities are also correlated in detail with the amount of intercalated L-proline and the reaction conditions. More interestingly and significantly, we found for the first time that the L-proline immobilized in the interlayers of LDHs keeps its optical activity and thus catalytic activity over thermal pretreatment.

2. Experimental

2.1. Preparation

All of the chemicals were of analytic grade and used as received. The Mg/Al–CO_3^{2-} LDHs precursors were synthesized by a method involving separate nucleation and aging steps [28]. Mg $(NO_3)_2{\cdot}6H_2O$ and Al $(NO_3)_3{\cdot}9H_2O$ with Mg^{2+}/Al^{3+} ratios of 2.0, 3.0, and 4.0 were dissolved in deionized water (225 mL) to give solutions with an Mg^{2+} concentration of 1.6 M. NaOH and Na_2CO_3 were dissolved in deionized water (225 mL) to form the mixed base solution. The concentrations of the base were related to the concentrations of metal ions: $[NaOH] = 1.6[Mg^{2+} + Al^{3+}]$ and $[CO_3^{2-}] = 2.0\ [Al^{3+}]$. The two solutions were simultaneously added to a colloid mill rotating at 3000 rpm and mixed for 2 min. The resulting slurry was removed from the colloid mill and aged at 373 K for 12 h. The final precipitate was filtered, washed thoroughly with deionized water, and dried at 373 K for 24 h.

The Mg/Al–CO_3^{2-} LDHs was calcined at 773 K for 5 h with a temperature-programmed rate of 5 K/min from room temperature to 773 K, and then naturally cooled, producing LDO.

L-Pro LDHs was prepared by the reconstruction of LDO in the solution of L-proline anion. The L-proline (0.756 g, 6 mmol) was dissolved in a freshly prepared solution of NaOH (6 mmol in 100 mL of deionized and decarbonated water), after which 0.5 g LDO (molar Mg/Al ratio = 3:1) was added. The resulting suspension was stirred (800 rpm) at 298 K for 24 h. All procedures were performed in a nitrogen atmosphere. The molar ratio of proline to Al was 2:1. The resulting precipitate was filtered, washed with deionized and decarbonated water twice and with ethanol once, and dried at 343 K for 10 h to obtain L-Pro LDHs. Changing the concentration of proline anion to 0.03 and 0.15 mol/L, the L-proline content was altered in L-Pro LDHs.

2.2. Characterization

Powder XRD patterns were obtained on a Shimadzu XRD-6000 instrument with Cu-K_α source, step size of 0.02°, and scan rate of 5°/min. In situ HTXRD measurements were carried out in a static air atmosphere between 298 and 873 K, after 15 min equilibration at each temperature; the sequential heating rate was 5 K/min. FTIR spectra were recorded in air on a Bruker Vector 22 spectrometer (resolution 4 cm^{-1}) in the range of 4000–400 cm^{-1}, the samples being pressed into disks with KBr crystal powder. C, N, and H elemental analyses were performed in an Elemental vario EL instrument, and metal elemental analyses were performed by ICP emission spectroscopy using solutions prepared by dissolving the samples in 10% dilute HNO_3. According to these data, the calculated intercalated yield is equal to $[C_5H_8NO_2]/[Al]$.

XPS spectra were obtained using a VG ESCALAB MK II spectrograph with Al$K\alpha$ radiation (15 kV, 15 mA), using 284.8 eV of C 1s in the same sample as the standard for the calculation of binding energy. The sensitivity factors used for compositional calculation were 0.42 for N and 0.25 for C.

Thermogravimetric analysis and differential thermal analysis (TG-DTA) were carried out on a custom-made PCT-1A thermal analysis system. The low-temperature N_2 adsorption–desorption experiments were carried out using a Quantachrome Autosorb-1 system. The sample was outgassed at 343 K for 2 h before measurement. The surface area of the L-Pro LDHs, using the BET method, was about 40 m^2/g, with a model pore diameter of 3.8 nm calculated using the BJH method based on the desorption isotherm.

2.3. Measurement

2.3.1. Thermal treatment on L-Pro LDHs

L-proline and L-Pro LDHs were heated for 2 h at 333, 373, 413, and 453 K and then subsequently dissolved in aqueous HCl (v/v = 1:1) with the volume made up to 20 mL with deionized water. The optical rotation was measured at room temperature using a 10-cm sample tube on a WZZ-IS automatic polarimeter at 589.3 nm (Na D-line).

2.3.2. UV irradiation on L-Pro LDHs

L-proline and L-Pro LDHs were exposed to UV light (200–380 nm, 250 W) for different periods. Then the samples were subsequently dissolved in aqueous HCl (v/v = 1:1) with the volume made up to 20 mL with deionized water. The optical rotation was measured as described above.

2.3.3. Catalytic testing

Aldol condensation reactions were performed in a closed 100-mL round-bottomed flask equipped with a mechanical stirrer. For a typical reaction (Scheme 1), benzaldehyde (1 mmol) and a certain amount of L-Pro LDHs catalyst (amounting to

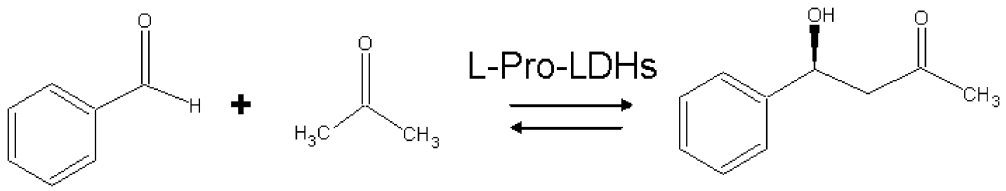

Scheme 1. The schematic representation of aldol reaction between benzaldehyde and acetone.

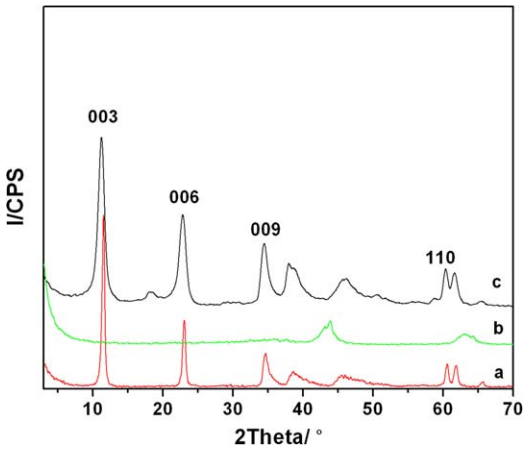

Fig. 1. XRD patterns for (a) Mg/Al–CO_3^{2-} LDH as precursor; (b) LDO; (c) L-Pro LDHs (molar ratio of Mg/Al = 3:1, intercalated yield = 59%).

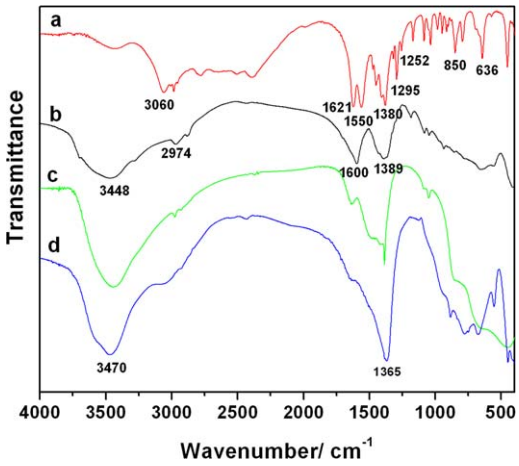

Fig. 2. FT-IR spectra for samples of (a) L-proline; (b) L-Pro LDHs (molar ratio of Mg/Al = 3:1, intercalated yield = 59%); (c) LDO; (d) Mg/Al–CO_3^{2-} LDH.

0.35 mmol L-proline in each case) were stirred in 1:4 acetone/solvent (acetone, dimethyl sulfoxide (DMSO), or heptane) at 313 K. Liquids were taken at regular intervals, and the product yield (%) was analyzed off-line on a Shimadzu GCMS-QP2010 instrument. At the same time, the ee (%) was determined by HPLC analysis using a chiralcel OB-H column (hexane/isopropanol = 90/10) with 254 nm UV light after vaporizing all of the acetone in the mixture solution and redissolving the product in 90/10 (v/v) hexane/isopropanol.

3. Results and discussion

3.1. Structural characterization

The XRD pattern of L-Pro LDHs prepared by the reconstruction method (molar ratio of Mg/Al = 3:1, intercalated yield = 59%) is shown in Fig. 1. For comparison, the XRD patterns of the Mg/Al–CO_3^{2-} LDHs and LDO as precursors are also shown in the figure. The main intense diffraction peaks of L-Pro LDHs appear at 11.27° (003), 22.82° (006), 34.45° (009), and 60.40° (110) with $d_{003} = 0.78$ nm, in accordance with a previous report on the intercalation of amino acids [33]. The appearance of these essential diffractions of LDHs expresses the successful reconstruction of the LDH structure. Subtracting the thickness of the LDHs layer (0.21 nm) and the hydrogen-bonding space (0.27 nm) [34], the interlayer gallery of L-Pro LDHs is estimated as 0.30 nm, equal to the thickness of L-proline (0.29 nm, calculated by ChemOffice 2004), suggesting an approximately horizontal orientation of interlayer L-proline anions with respect to the hydroxide layers. In comparison with the Mg/Al–CO_3^{2-} LDHs as precursor, however, the (*hkl*) reflections shift slightly to a lower degree and the interlayer space of the (003) plane increases by only 0.02 nm. Therefore, the intercalation of proline requires further confirmation by FTIR and elemental analysis.

The FTIR spectra for the Mg/Al–CO_3^{2-} LDHs as precursor, LDO, L-Pro LDHs (molar ratio of Mg/Al = 3:1, intercalated yield = 59%), and pristine L-proline are illustrated in Fig. 2. The bands (Fig. 2a) at 3070–2350 cm^{-1} correspond to the asymmetric stretching vibration and the bending vibration of the N–H groups in L-proline. The bands at 1621, 1550, and 1380 cm^{-1} are assigned to the –COOH group. The absorption bands of the C–N and C–C bonds appear at 1295 and 1252 cm^{-1}, respectively. The bands at 850–600 cm^{-1} are bending C–H vibration bands. The broad band at around 3448 cm^{-1} (Fig. 2b) is due to hydrogen bonding of interlayer water and interlayer anions with the hydroxyl groups on the layers, which are found at lower frequency compared with the O–H bond stretch at around 3600 cm^{-1} in pure water. The bands around 2974 cm^{-1} correspond to the asymmetric stretching vibration of the N–H and C–H groups. The bands at 1600 and 1389 cm^{-1} are related to the asymmetric stretching mood of the $–COO^-$ groups, proving the existence of L-proline as interlayer anions in the sample, and supporting the XRD results. However, the vibration absorption band of carbonates at 1365 cm^{-1} (Fig. 2d) is possibly overlapped by the asymmetric stretching mode of the $–COO^-$ group at 1389 cm^{-1}. The bands centered at 822 and 629 cm^{-1} (Fig. 2b) are due mainly to the crystal lattice vibration of Mg–O and Al–O bonds, as well as the stretching and bending deformation M–O–M and O–M–O vibrations.

Table 1
Chemical composition of different Mg/Al L-Pro LDHs

Molar ratio of Mg/Al[a]	Molecular formula	N content (g/g)	Proline content[b] (mmol/g)	Intercalated yield[c]
2:1	$Mg_{4.18}Al_{2.00}(OH)_{12}(C_5H_8NO_2)_{1.05}(CO_3)_{0.47}\cdot 3.90H_2O$	2.6%	1.8	53%[d]
3:1	$Mg_{6.33}Al_{2.00}(OH)_{16}(C_5H_8NO_2)_{0.59}(CO_3)_{0.71}\cdot 4.07H_2O$	1.2%	0.9	30%
3:1	$Mg_{6.33}Al_{2.00}(OH)_{16}(C_5H_8NO_2)_{1.02}(CO_3)_{0.49}\cdot 4.07H_2O$	2.0%	1.5	51%
3:1	$Mg_{6.33}Al_{2.00}(OH)_{16}(C_5H_8NO_2)_{1.18}(CO_3)_{0.41}\cdot 4.07H_2O$	2.3%	1.7	59%[d]
4:1	$Mg_{8.24}Al_{2.00}(OH)_{20}(C_5H_8NO_2)_{1.32}(CO_3)_{0.34}\cdot 4.02H_2O$	2.2%	1.6	66%[d]

[a] Millimolar L-proline anion in per gram of different Mg/Al L-Pro LDHs.
[b] Intercalated yield = $[C_5H_8NO_2]/[Al]$.
[c] Mg/Al molar ratio in the synthesis mixture.
[d] The maximum content of intercalated L-proline anions.

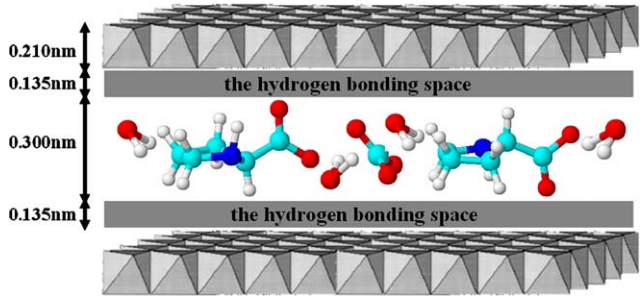

Fig. 3. The schematic model of L-Pro LDHs (molar ratio of Mg/Al = 3:1, intercalated yield = 59%).

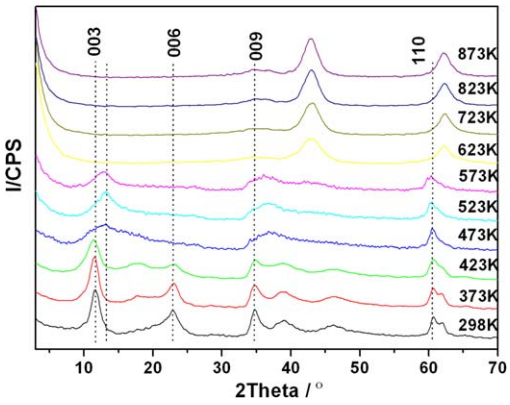

Fig. 4. In situ HTXRD patterns of L-Pro LDHs (molar ratio of Mg/Al = 3:1, intercalated yield = 59%) from 298 to 873 K.

The chemical composition based on ICP and C, H, and N elemental analysis of the L-Pro LDHs with different contents of the interlayer L-proline anions is given in Table 1. The L-proline content shown in Table 1 is much higher than the 0.225 mmol/g for L-Pro LDHs prepared using the ion-exchange method [23], indicating that the L-proline anions have been incorporated into the interlayer galleries rather than being located at the edges observed by Choudary et al. [23]. The XPS analysis for L-Pro LDHs (molar ratio of Mg/Al = 3:1, intercalated yield = 59%) shows a surface N content of 2.3%, approaching the content of 2.3% in the bulk shown in Table 1, confirming the intercalation of the L-proline anions into the LDH interlayer galleries as opposed to simple absorption on the external surface.

In addition to the L-proline anions, some carbonate anions are also co-intercalated within the interlayer gallery. The co-intercalation of carbonate is required by balancing the positive charge of the LDH layers, because monovalent L-proline anions in only a horizontal orientation cannot balance the charges due to spatial restrictions. It can also be seen from Table 1 that the L-proline content in L-Pro LDHs samples was successfully altered by one of two approaches: changing the concentration of L-proline as guest or changing the Mg/Al molar ratio of the mixed oxide as host.

Based on the above results and discussions, the structural model for L-Pro LDHs (molar ratio of Mg/Al = 3:1, intercalated yield = 59%) is given in Fig. 3. The model shows the L-proline anions in an approximately horizontal orientation with respect to the hydroxide layers, with the carboxylate groups attaching directly to hydroxide layers [35] containing four water molecules and one carbonate. The interlayer water molecules alternately with the L-proline anions promote hydrogen bonding with the hydroxide layers [36], which may have a significant effect on the catalytic activity of the L-Pro LDHs.

3.2. Stability of the l-Pro LDHs

3.2.1. Thermal stability

3.2.1.1. In situ HTXRD The in situ HTXRD patterns of L-Pro LDHs (molar ratio of Mg/Al = 3:1, intercalated yield = 59%) in ambient atmosphere are given in Fig. 4 through some repetitive treatments consisting of calcinations at increasing temperatures. Three steps are observed in the thermal decomposition process in the temperature ranges $298 \leqslant T \leqslant 473$ K, $473 \leqslant T \leqslant 623$ K and $623 \leqslant T \leqslant 873$ K. In the first step, the basal spacing d_{003} decreases from 0.768 nm at 298 K to 0.695 nm at 573 K (Fig. 5), related to the destruction of hydrogen bonding as a result of the desorption of the surface adsorbed water and deintercalation of interlayer water molecules. This provides supporting evidence for the structural model of L-Pro LDHs discussed above. However, there is an abnormal rise in the basal spacing d_{003} around 423 K. We suggest that along with the loss of the interlayer water molecules and the dielectric coefficient of water, a strengthening of the electrostatic force between the L-proline anions and the hydroxide layers occurs, resulting in a transformation in the arrangement gradient of interlayer proline anions. In the second step, a further decrease in the value of d_{003} is observed with continuous heating, which can be attributed to the decomposition of interlayer carbonate anions and the dehydroxylation of the brucite

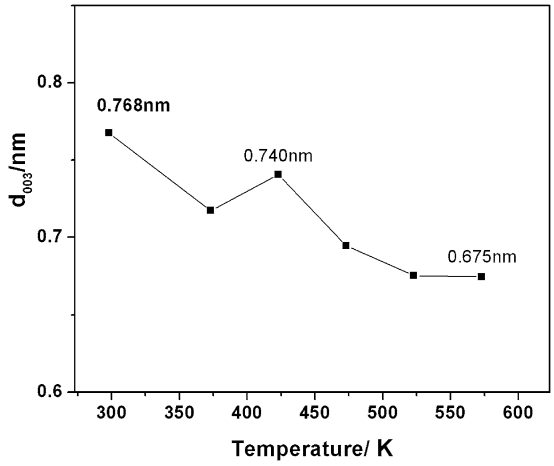

Fig. 5. The relationship between d_{003} basal spacing of L-Pro LDHs (molar ratio of Mg/Al = 3:1, intercalated yield = 59%) and temperature.

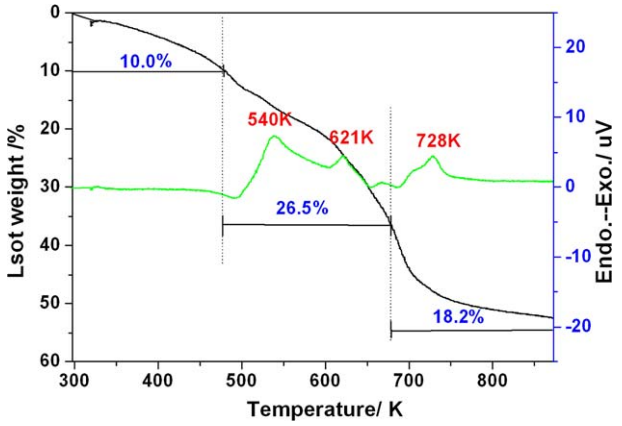

Fig. 6. The TG-DTA curves for L-Pro LDHs (molar ratio of Mg/Al = 3:1, intercalated yield = 59%).

layers, as well as the bond-breaking of L-proline anions. The layered structure collapses completely at 623 K with the appearance of the reflection characteristic of LDO at 42.91° and 62.32° after the dehydroxylation of the host layers from 573 to 623 K. In the final step above 623 K, along with the continuous dehydroxylation of the host layers, the intensity of the LDO diffractions becomes stronger due to the change in the chemical environment of the Al from the exclusively octahedral coordination.

3.2.1.2. TG-DTA The TG-DTA curves of the L-Pro LDHs (molar ratio of Mg/Al = 3:1, intercalated yield = 59%) show three steps of thermal decomposition (Fig. 6), similar to the in situ HTXRD patterns. The first one, from room temperature to 473 K (weight loss = 10.0%), corresponds to removal of the surface-adsorbed water and interlayer water molecules, which is in good agreement with the first step of in situ HTXRD patterns. The weight loss approximates the water content of 10.3% calculated from the elemental analysis. The second step, in the temperature range of 473–673 K, involves the decomposition of interlayer carbonate anions and the dehydroxylation of the brucite layers, as well as the bond-breaking of L-proline anions,

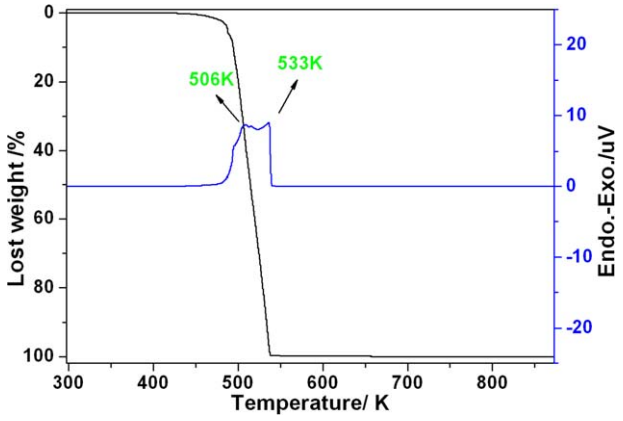

Fig. 7. The TG-DTA curves for L-proline.

which is actually consistent with the results of in situ HTXRD. The exothermic peaks are located at 540 and 621 K, respectively, and the weight loss (26.5%) in this period is close to the total mass percentage (23.7%) of interlayer carbonate anions and the hydroxyl groups released in form of carbon dioxide and water molecules. The final process is assigned to the deep combustion of the interlayer proline anions corresponding to the exothermic peak at 728 K, with the weight loss of 18.2% approaching the residues of L-proline anions (19.3%) until formation of the LDO. Compared with the TG-DTA curves of pristine L-proline (Fig. 7), which show the complete decomposition of L-proline below 537 K, the thermal stability of L-proline has been largely promoted via the immobilization by LDHs.

3.2.2. Optical stability on thermal treatment and UV radiation

Generally, the chiral amino acids are sensitive to heat, light radiation, strong acidic or basic media, and aldehyde media [37,38]. As a consequence, the optical activity of chiral amino compounds is usually lost during their immobilization, storage, delivery, and application processes [39]. However, in our experiments, the specific optical rotation of L-proline anions (−50.5°) after releasing the interlayer L-proline anions was quite close to that of the pristine L-proline (−52.5°), indicating that the optical activity of L-proline was maintained during the intercalated process.

The optical stability of L-Pro LDHs (molar ratio of Mg/Al = 3:1; intercalated yield = 59%) was also studied in detail under the conditions of thermal treatments and UV irradiation. The influence of thermal treatment on the optical activity is illustrated in Fig. 8. Pristine L-proline was also investigated for comparison. It is clear that the specific optical rotation of L-proline itself decreases drastically from −51.50° to −39.00° with increasing temperature (Fig. 8a), while that of the L-Pro LDHs decreases by only −1.00° (Fig. 8b) under the same conditions. According to the TG-DTA curves (Figs. 6 and 7), L-proline is stable below 453 K, proving that the loss of optical activity in this experiment is due to racemization rather than to decomposition. The optical changes in L-proline and L-Pro LDHs (molar ratio of Mg/Al = 3:1, intercalated yield = 59%) under UV radiation are shown in Fig. 9, indicating results similar to those for thermal treatment.

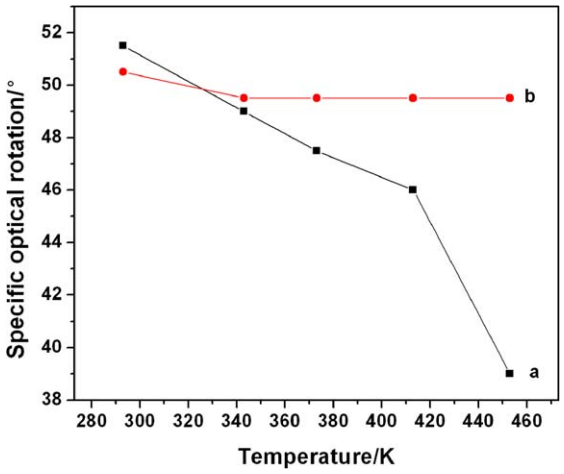

Fig. 8. The relationship between specific optical rotation and thermal treatment temperature of (a) L-proline; (b) L-Pro LDHs (molar ratio of Mg/Al = 3:1, intercalated yield = 59%).

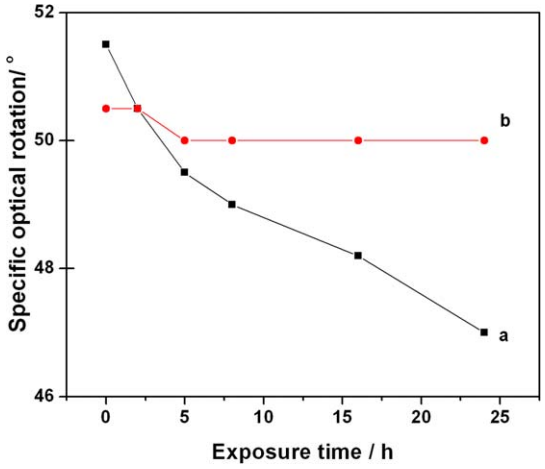

Fig. 9. The relationship between specific optical rotation and exposure time under UV radiation of (a) L-proline; (b) L-Pro LDHs (molar ratio of Mg/Al = 3:1, intercalated yield = 59%).

The stabilization of optical activity for L-Pro LDHs might be attributed to the restriction or confinement of the host galleries to the transformation of stereo configuration of the chiral guest [40]. The obstruction of light penetration by the LDH slabs can also account for this improvement under UV irradiation. Therefore, the immobilization of L-proline on LDHs significantly inhibits the racemization of L-proline anions, effectively enhancing the optical stability.

3.3. Catalytic performance

3.3.1. The catalytic mechanism

The possible catalytic mechanism of the direct aldol reaction between acetone and benzaldehyde, in which the L-Pro LDHs functions as the heterogeneous catalyst, based on the homogeneous enamine mechanism, is illustrated in Scheme 2 [41]. In the homogeneous system, List et al. [42] and Houk et al. [43] investigated the enamine mechanism involving single proline molecule and found it to be more convincing than the previous one [44]. The proline was considered to function as a "micro-aldolase" that provided both the nucleophilic amino group and an acid/base co-catalyst in the form of the carboxylate [42,45]. A later investigation by Rankin et al. [46] appended the effect of solvent. According to the homogeneous mechanism described above, we propose a heterogeneous mechanism (Scheme 2). First, the acetone and benzaldehyde molecules diffuse into the interlayer space to contact the interlayer L-proline anions (step 1). Moreover, the interlayer species, i.e. the water molecules, carbonate, and L-proline anions, hoppingly diffuse within the galleries [47,48], further facilitating the contact between the reactants and L-proline anions. Subsequently, the whole catalytic process occurs mainly inside the interlayer space. The initial nucleophilic attack of the amino groups to the acetone and the subsequent dehydration process generate a carbinol amine intermediate **a**, which balances the positive charges on the layers (step 2). For the refacial attack of benzaldehyde to the intermediate **a** [49] on the way to the transition state **b**, two oxygen atoms are attached to the hydroxide layer (step 3). The transition state **b** undergoes a hydrolysis process to yield the aldol product **c** [(4*R*)-hydroxy-4-phenyl-butan-2-one], releasing the L-proline anions (step 4). Finally, the product **c** diffuses out of the interlayers, achieving one catalytic cycle (step 4). The enantioselectivity can be explained by a metal-free version of a Zimmerman–Traxler-type transition state [50]. It is proposed that on the one hand, confinement of the galleries leads to the slowed aldol reaction due to the addition of the diffusion process, and on the other hand, the participation of the hydroxide layers in the catalytic process not only accelerates the formation of the enamine intermediate, but also promotes the enantioselectivity due to the oriented attack. However, the concrete roles of the LDHs on L-proline in the aldol reaction require more evidence, and investigations are currently underway in our lab.

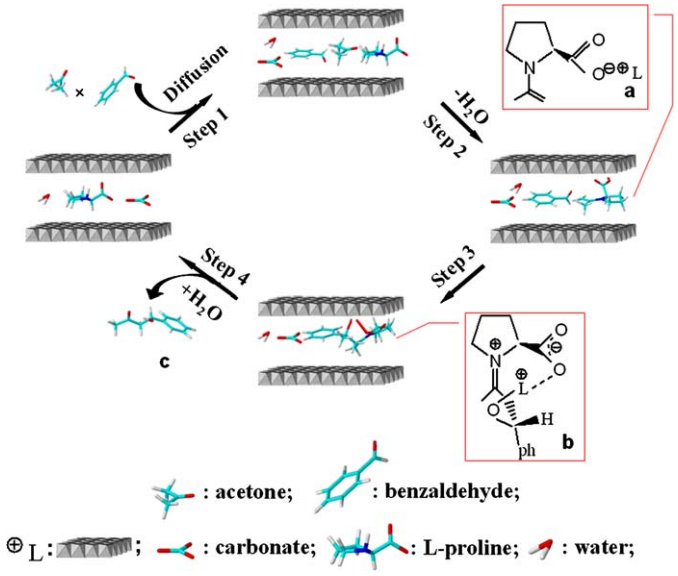

Scheme 2. The schematic representation of the mechanism of aldol reaction between benzaldehyde and acetone.

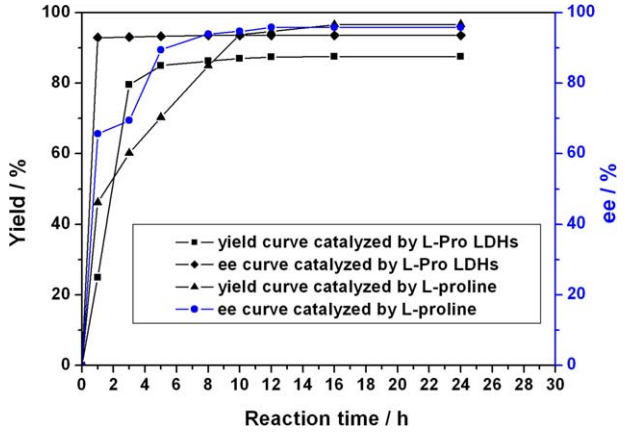

Fig. 10. The relationship between the yield/ee and reaction time catalyzed by L-Pro LDHs (molar ratio of Mg/Al = 3:1, intercalated yield = 59%) and L-proline.

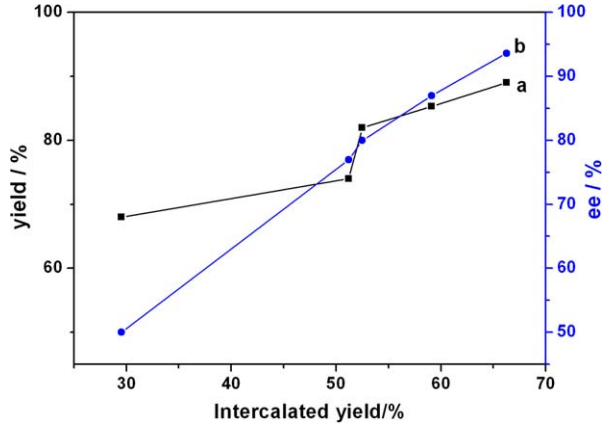

Fig. 11. The relationship between the yield (a) and ee (b) in aldol reaction and the intercalated yield of L-proline in L-Pro LDHs.

Table 2
The yield and ee of different reaction conditions in aldol reaction catalyzed by L-Pro LDHs

Catalysts	Reaction conditions		Yield (%)	ee (%)
	Solvent	Temperature (K)		
L-Pro LDHs (Mg/Al = 3:1, intercalated yield = 59%)	Acetone	293	80	93
	Acetone	313	88	94
	Acetone	Boiling point	89	94
	Heptane	313	22	62
	DMSO	313	63	87

3.3.2. *Effect of reaction conditions on catalytic activity*

The relationship between the yield/ee and reaction time catalyzed by L-Pro LDHs (molar ratio of Mg/Al = 3:1; intercalated yield = 59%) and L-proline demonstrates that the aldol reaction catalyzed by L-Pro LDHs attains a steady yield of 88% and an ee of 94% at 8 h (Fig. 10). Therefore, in further studies, 8 h was selected as a sufficiently short reaction period for termination of the catalytic process. Commonly, immobilization of the homogeneous catalyst causes a marked decrease in the catalytic activity. However, the yield and ee for the L-Pro LDHs are just a little lower than those in the homogeneous system (yield of 95% and ee of 96%, close to those reported by Gröger and Wilken [49]). That means that the immobilization on LDH has no adverse effect on the catalytic activity of L-proline in the asymmetric aldol reaction. Moreover, the reaction rate catalyzed by L-Pro LDHs is much faster (Fig. 10). This can be related to the easier formation of the carbinol amine intermediate (see Scheme 2) on L-Pro LDHs, because the proline anions are more nucleophilic than nonionized L-proline in attacking the acetone. It can also be deduced that the controlling reaction step is probably the nucleophilic attack of the amino group to the reactants.

Both product yield and ee are affected by the reaction temperature (Table 2). At 293 K, the product yield is 90% and the ee is 94%. At higher temperatures, such as the boiling point, the product yield and ee are both 90%. The higher reaction temperature can on the one hand promote conversion of the reactants and on the other hand lead to the racemization of the product so as to cause a small decrease in ee.

The role of the solvent was also found to be important, as shown in Table 2. When the reaction was performed with 1:4 acetone/solvent (DMSO or heptane) at 313 K, a higher yield was observed in DMSO (63%) than in heptane (22%). The hydrophilic LDHs show a stronger affinity to the polar solvents. Therefore, the stronger polarity of DMSO makes it possible to accelerate the diffusion process of the reactants, giving rise to a higher reaction yield. In the case of acetone, besides the strong polarity of the acetone as solvent, the excess of acetone as reactant makes it easy for the aldol reaction to proceed at completion, attaining a yield of 88% and an ee of 94% at 313 K.

3.3.3. *Effect of chemical composition on catalytic activity*

The L-proline content in the L-Pro LDHs catalysts was successfully tailored (as illustrated in Table 1) to investigate the effect of active site content on the catalytic reactions. Fig. 11 shows the effect of L-proline content on the product yield and ee catalyzed by L-Pro LDHs. The more guests intercalated, the higher the yield and ee achieved. The yield and ee reach 89 and 94%, respectively, for L-Pro LDHs with intercalated yields of 66%.

We also studied the catalytic activity of L-Pro LDHs (molar ratio of Mg/Al = 2:1; intercalated yield = 53%) with varying water content. The water content was altered by vacuum pumping. The yield and ee curves, shown in Fig. 12, both exhibit a steep change at a water content of 1.5% and decrease sharply with increased water content from 0.2 to 1.5%. The catalytic activity of the L-Pro LDHs changes only slightly when the water content is $>1.5\%$. The XRD measurement indicates that, as opposed to the high-temperature treatment, no decrease occurs in the d_{003} basal spacing of L-Pro LDHs under vacuum pumping. Thus, the loss of the interlayer water molecules results in a decrease in the spatial hindrance and thus an increase in the void space between the L-proline anions, accounting for the steep increment in the yield and ee at a water content of $\leqslant 1.5\%$. The interlayer water content affects the catalytic activity and enantioselectivity of the L-Pro LDHs more significantly than the absorbed water.

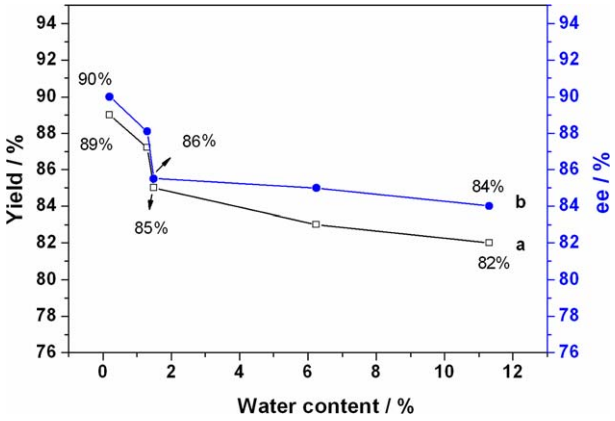

Fig. 12. The relationship between the yield (a) and ee (b) and the water content.

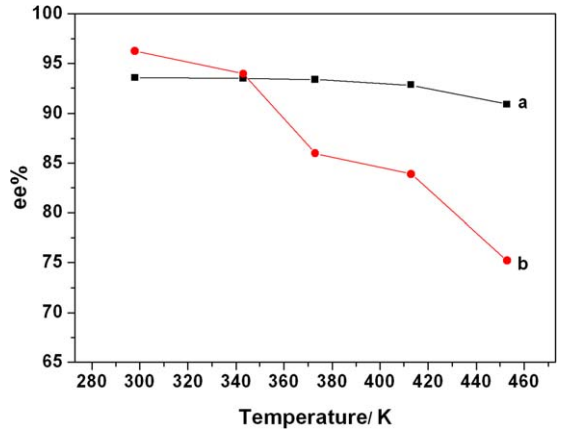

Fig. 13. The relationship between ee and treatment temperature of (a) L-Pro LDHs (molar ratio of Mg/Al = 3:1, intercalated yield = 59%) and (b) L-proline.

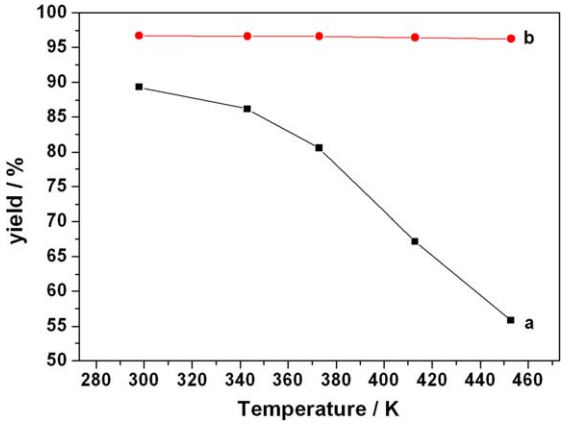

Fig. 14. The relationship between yield and treatment temperature of (a) L-Pro LDHs (molar ratio of Mg/Al = 3:1, intercalated yield = 59%) and (b) L-proline.

3.3.4. Catalytic activity and optical stability

Section 3.2.2 compared the optical stability against thermal treatment of L-Pro LDHs (molar ratio of Mg/Al = 3:1; intercalated yield = 59%) and pristine L-proline. Here the resulting products were taken as the catalysts in the aldol reaction. As shown in Figs. 13 and 14, along with the increasing pretreatment temperature, the yield and ee change in different ways on the L-Pro LDHs and L-proline. When the temperature increases from 298 to 453 K, the ee decreases slightly (from 94 to 91%) for L-Pro LDHs, but decreases sharply (from 96 to 75%) for L-proline (Fig. 13a). This discrepancy is attributed to the different optical stability on thermal treatment of L-Pro LDHs and L-proline. The immobilization markedly enhances the optical stability of L-proline (Fig. 8), contributing to the stabilization of enantioselectivity according to the catalytic mechanism discussed above. In contrast, the product yield catalyzed by L-Pro LDHs decreases sharply (from 90 to 56%) with increasing pretreatment temperature, whereas the yield on L-proline remains unchanged. There are two possible explanations for this result. As observed from in situ HTXRD patterns (Fig. 6), the d_{003} basal spacing decreases with the increment in thermal treatment temperature, obviously due to the loss of interlayer water molecules. The decrease in the interlayer spacing intensifies the spatial hindrance to the diffusion process, resulting in reduced catalytic activity (Scheme 2). On the other hand, with the removal of the interlayer water molecules, the electrostatic force between the L-proline anions and the hydroxide layers is strengthened. Thus, the catalytic activity of the L-Pro LDHs declines sharply due to the lower mobility of proline anions. The stabilization of enantiomeric selectivity on thermal treatment gives L-Pro LDHs advantages in storage, delivery, and application processes.

4. Conclusion

In summary, the reconstruction method based on the "memory effect" of Mg–Al LDHs has proven to be an effective means of achieving intercalation of L-proline anions. Moreover, the proline content can be tailored in a certain range. Applying L-Pro LDHs in the aldol reaction reveals that the immobilization on LDHs has no adverse effect on the catalytic activity of L-proline. In addition, immobilization by LDHs can effectively prevent the racemization of L-proline under both thermal treatment and UV irradiation. Thus L-Pro LDHs as a heterogeneous asymmetric catalyst in aldol reactions exhibits high enantioselectivity even when exposed to rigorous conditions. This novel solid catalyst has several advantages, including high activity under mild liquid-phase conditions, ready separability by simple filtration, and lack of side products and thus eco-friendliness.

Acknowledgments

The authors are grateful for financial support from the NSFC (20473008 and key project 20531010) and the Program for New Century Excellent Talents in University (NCET). They thank Professor X. Duan for helpful discussions.

References

[1] H. Torri, M. Nakadai, K. Ishihara, S. Saito, H. Yamamoto, Angew. Chem. Int. Ed. 43 (2004) 1983.
[2] M. Shibasaki, H. Sasai, T. Arai, Angew. Chem. Int. Ed. Engl. 36 (1997) 1236.
[3] S. Matsukawa, N. Okano, T. Imamoto, Tetrahedron Lett. 41 (2000) 103.

[4] B. List, P. Pojarliev, C. Castello, Org. Lett. 3 (2001) 573.
[5] L. Hoang, S. Bahmanyar, K.N. Houk, B. List, J. Am. Chem. Soc. 125 (2003) 16.
[6] K. Sakthivel, W. Notz, T. Bui, C.F. Barbas III, J. Am. Chem. Soc. 123 (2001) 5260.
[7] D. Tichit, D. Lutic, B. Coq, R. Durand, R. Teissier, J. Catal. 219 (2003) 167.
[8] A. Córdova, W. Notz, G.F. Zhong, J.M. Betancort, C.F. Barbas, J. Am. Chem. Soc. 124 (2002) 1842.
[9] H. Groger, E.M. Vogel, M. Shibasaki, Chem. Eur. J. 4 (1998) 1137.
[10] M. Movassaghi, E.N. Jacobsen, Science 298 (2002) 1904.
[11] Z.G. Hajos, D.R. Parrish, J. Org. Chem. 39 (1974) 1615.
[12] E.R. Jarvo, S.J. Miller, Tetrahedron 58 (2002) 2481.
[13] K. Nakamura, R. Yamanka, T. Matsuda, T. Harada, Tetrahedron: Asymmetry 14 (2003) 2659.
[14] W. Hotz, F. Tanaka, C.F. Barbas III, Acc. Chem. Res. 37 (2004) 580.
[15] K.R. Knudsen, E.T. Mitchell, V.L. Steven, Chem. Commun. (2006) 66.
[16] J. Wang, H. Li, Y. Mei, B. Lou, D. Xu, D. Xie, H. Guo, W. Wang, J. Org. Chem. 70 (2005) 5678.
[17] P. Dambruoso, A. Massi, A. Dondoni, Org. Lett. 7 (2005) 4657.
[18] Q.H. Xia, H.Q. Ge, C.P. Ye, Z.M. Liu, K.X. Su, Chem. Rev. 105 (2005) 1603.
[19] S.J. Bae, S.W. Kim, T. Hyeon, B.M. Kim, Chem. Commun. (2000) 31.
[20] S.W. Kim, S.J. Bae, T. Hyeon, B.M. Kim, Microporous Mesoporous Mater. 44–45 (2001) 523.
[21] H.M.L. Davies, C. Venkataramani, T. Hansen, D.W. Hopper, J. Am. Chem. Soc. 125 (2003) 6462.
[22] H.M.L. Davies, A.M. Walji, Org. Lett. 5 (2003) 479.
[23] B.M. Choudary, B.K. Avita, C.N. Sreenivasa, B. Sreedhar, K.M. Lakshmi, Catal. Lett. 78 (2002) 373.
[24] A. Drits, T.N. Sokolova, G.V. Sokolova, V.I. Cherkashin, Clays Clay Miner. 35 (1987) 401.
[25] D. Walsh, B. Lebeau, S. Mann, Adv. Mater. 11 (1999) 324.
[26] A. Corma, V. Fornés, R.M. Martín-Aranda, F. Rey, J. Catal. 134 (1992) 58.
[27] S.H. Han, C.G. Zhang, W.G. Hou, D.J. Sun, G.T. Wang, Colloid Polym. Sci. 274 (1996) 860.
[28] Y. Zhao, F. Li, R. Zhang, D.G. Evans, X. Duan, Chem. Mater. 14 (2002) 4286.
[29] A.P. Mariko, F. Claude, J.P. Besse, J. Mater. Chem. 13 (2003) 1988.
[30] S. Abelló, F. Medina, D. Tichit, J.P. Ramírez, J.C. Groen, J.E. Sueiras, P. Salagre, Y. Cesteros, Chem. Eur. J. 11 (2005) 728.
[31] S. Carlino, M.J. Hudson, S.W. Husain, J.A. Knowles, Solid State Ionics 84 (1996) 117.
[32] J. He, M. Wei, B. Li, Y. Kang, D.G. Evans, X. Duan, Struct. Bond. 119 (2005) 89.
[33] H. Nakayama, N. Wada, M. Tsuhako, Int. J. Pharm. 269 (2004) 469.
[34] V. Prevot, C. Forano, J.P. Besse, F. Abraham, Inorg. Chem. 37 (1998) 4293.
[35] S.P. Newman, S.J. Williams, P.V. Coveney, W. Jones, J. Phys. Chem. B 102 (1998) 6710.
[36] S.P. Newman, T.D. Cristina, V. Coveney, W. Jones, Langmuir 18 (2002) 2933.
[37] R. Griffith, J. Soria, J.G. Wood, Exp. Neurol. 161 (2000) 297.
[38] M. Shinitizky, F. Nudelman, Y. Barda, R. Haimovitz, E. Chen, D.W. Deamer, Origins Life Evol. B 32 (2002) 285.
[39] R.N. Patel, R.L. Hanson, A. Banerjee, L.J. Szarka, J. Am. Oil Chem. Soc. 74 (1997) 1345.
[40] M. Wei, Q. Yuan, D.G. Evans, Z.Q. Wang, X. Duan, J. Mater. Chem. 15 (2005) 1197.
[41] C. Allemann, R. Gordillo, F.R. Clemente, P.H.-Y. Cheong, K.N. Houk, Acc. Chem. Res. 37 (2004) 558.
[42] L. Hoang, S. Bahmanyar, K.N. Houk, B. List, J. Am. Chem. Soc. 125 (2003) 16.
[43] S. Bahmanyar, K.N. Houk, J. Am. Chem. Soc. 123 (2001) 11273.
[44] C. Agami, C. Puchot, J. Mol. Catal. 38 (1986) 341.
[45] B. List, R.A. Lerner, C.F. Barbas III, J. Am. Chem. Soc. 122 (2000) 2395.
[46] K.N. Rankin, J.W. Gauld, R.J. Boyd, J. Phys. Chem. A 106 (2002) 5155.
[47] J.W. Wang, A.G. Kalinichev, R.J. Krikpatrick, X.Q. Hou, Chem. Mater. 13 (2001) 145.
[48] X.Q. Hou, R.J. Kirkpatrick, Chem. Mater. 12 (2000) 1890.
[49] H. Gröger, J. Wilken, Angew. Chem. Int. Ed. 40 (2001) 529.
[50] H.E. Zimmerman, M.D. Traxler, J. Am. Chem. Soc. 79 (1957) 1920.